Current Topics in Electrochemistry
Vol. 22, 2020

Original Article

Comparison of 3D-carbon felt and 2D-carbon cloth for the bioremediation of acetaminophen using *Trichoderma harzianum* biofilm versus mixed biofilm of *Trichoderma harzianum/Pseudomonas fluorescens* in a fungal microbial fuel cell

Mehri Shabani[1,2,*,#], Maxime Pontié[1,*,$], Habibollah Younesi[2] and Marwa Jaidi[3]

[1]University of Angers, Faculty of Science, Department of Chemistry, Group Analysis and Processes, 2 Bd. Lavoisier, F-49045 Angers cedex 01, France. [2]Tarbiat Modares University, Department of Environmental Science, Faculty of Natural Resources, Tehran, Iran.
[3]National Engineering Schooll of Sfax, Department of Biological Engineering, Sfax, Tunisia.

ABSTRACT

Three-dimensional (3D) carbon felt was compared with two-dimensional (2D) carbon cloth in terms of their efficiency for application in a fungal microbial fuel cell to biodegrade acetaminophen (APAP). A solution of 300 mgL^{-1} of APAP was used in the anode compartment that played the role of carbon source for microorganisms. The study also aimed to investigate the efficiency of both pure fungal biofilm of *Trichoderma harzianum* versus a mixed biofilm of *Trichoderma harzianum/ Pseudomonas fluorescens* in biodegradation APAP. The results revealed that 3D-carbon felt (CF) was able to provide a higher amount of power density of 0.13 mW m^{-2} and 1.7 mW m^{-2} both in pure and mixed biofilm, respectively On the other hand, almost 10 times lower power density values were achieved with systems using 2D-carbon cloth (CC) vs 3D- carbon felt (CF). From this standpoint, both systems employing mixed biofilm can be considered more efficient in terms of faster degradation of APAP with lower half-life time, regardless of the electrode type. Additionally, the 3D-carbon felt colonized by a mixed biofilm of fungal-bacterial showed at least 3 times higher biodegradation kinetic rate than the 2D-carbon cloth.

KEYWORDS: 3D-carbon felt, 2D-carbon cloth, APAP biodegradation, MFC, power density.

ABBREVIATIONS

APAP	=	acetaminophen
CF	=	carbon felt
CC	=	carbon cloth
CFU	=	colony forming unit
FMFC	=	fungal microbial fuel cell
GCE	=	glassy carbon electrode
MFC	=	microbial fuel cell
NAPQI	=	N-acetyl-p-benzoquinone imine
PAP	=	para-aminophenol
PBS	=	phosphate buffer solution
PCT	=	paracetamol
SCE	=	saturated calomel electrode
UP	=	ultrapure
KeV	=	kiloelectron volt(s)

1. INTRODUCTION

Pharmaceutical contamination has been recently emerging as a threat to water resources. Despite their low level of concentration, they are considered hazardous due to their accumulation in living tissues

*Email id: [$]maxime.pontie@univ-angers.fr; [#]shabani.mehri@gmail.com

and further ecological effects on the population [1]. Pharmaceuticals are released into the environment through improper disposal, runoff, and leakage from the sewer pipes. Among these, acetaminophen (APAP), also known as paracetamol (PCT), is a widely used over-the-counter analgesic and antipyretic. Hence, due to its widespread consumption, it has become one of the environmental concerns over the years. It is reported that 90 percent of APAP is removed in wastewater treatment plants [2] but considering its negative impact and to control disposal risks, an environmentally friendly approach with high efficiency is still missing.

Biological degradation is one of the promising methods to degrade APAP due to its efficient, safe, short, easy, and environmentally friendly approach. It has been proved that microorganisms play an important role in APAP degradation under various conditions [3, 4]. The use of fungal microbial fuel cells (FMFC) is a low cost and suitable bioprocess that utilize the microorganisms as bioanodes for pollution removal simultaneously with the production of clean energy [5, 6]. An FMFC consists of two compartments of anode and cathode. The anode chamber contains microorganisms utilized to degrade pollutants, whereas the cathode chamber is a place of oxygen reduction [7]. Generally, as the anode, carbon materials could improve the interfacial microorganism colonization and speed up the development of extracellular biofilms, which increases power density produced by the electron transfer [8].

Carbon materials as the bioanodes could have two-dimensional (2D) or three-dimensional structures (3D) such as carbon cloth (2D), carbon felt, graphite, carbon foam, and carbon tube (3D). There are pieces of evidence that 3D materials showed higher efficiency when used as bioanodes [9-11]. A series of recent studies have indicated that 3D materials led to more efficient bioanodes for various applications [10, 12-14]. There is also a study dedicated to comparing the 2D and 3D structures as bioanodes, which is directly related to our study in terms of material choice [15]. Further studies are essential to fill this gap in the scientific literature, and hence this paper addresses the need for a direct comparison of performance between 2D-carbon cloth and 3D-carbon felt used in microbial fuel cells with the aim of bioremediation and electricity generation.

The present study aimed to compare the suitability and performance of 2D-carbon cloth (CC) and 3D-carbon felt (CF) as bioanodes. The bioelectrochemical degradation of APAP using various bioanodes has been rarely investigated. Herein, we applied two systems including, 1) the pure fungal culture of *Trichoderma harzianum*, and 2) the mixed bacterial-fungal culture of *Trichoderma harzianum*/*Pseudomonas fluorescens*, to investigate the degradation of the APAP. The electrochemical method was employed to follow the degradation of APAP in an FMFC, where we investigated the FMFC performances in terms of power density. Authors have also compared the performance of FMFCs in terms of obtained power density by applying the various electrodes.

2. MATERIALS AND METHODS

2.1. Reagents and strains

APAP was provided by Sigma-Aldrich (France). All aqueous solutions were prepared from analytical grade chemicals and deionized water with a pH of 6.5, conductivity <1 mS cm^{-1}, and TOC <0.1 mg L^{-1} (Elga Lab Water ultrapure-water system, Purelab-UV-UF, Elga) was used. A phosphate buffer solution (0.1 M PBS) of pH 7.2 was used as a supporting electrolyte with APAP. *Trichoderma harzianum* was isolated from wood samples in the vicinity of Angers (France) and was provided by IRHS-INRAE Angers research center, France (n°1573). *Trametes Versicolor* was isolated from a stump of Landes pine in the vicinity of Source-Hossegor (France) and used to colonize the cathode. *Pseudomonas fluorescens* was isolated from dam water samples of St Nicolas's dam in Angers (France) and routinely maintained at 4 °C on a Colombia agar medium supplied by Thermo Fisher Scientific (France).

2.2. FMFC construction and operation

We follow the FMFC structure reported earlier [6]. The FMFC was made of two compartments of bioanode and biocathode separated by a membrane. The bioanode compartment contained 300 mg L^{-1} APAP in PBS (0.1 M phosphate buffer pH=7.4) solution and microorganisms responsible for the biodegradation, which resulted in the production of electrons and protons. The generated electrons flow through an external circuit using the electrodes

(CF and CC), while the protons passed through a cationic exchange membrane to the cathode. The movements of electrons produce current/power. In the present study, an external resistor was connected to the electrodes in order to cause electrons to move from anode to cathode. The aerated biocathode compartment contained PBS solution and *Trametes versicolor* to catalyze the oxygen reduction. The aeration was conducted using a 0.45 μm filter connected to an air pump.

The authors applied a novel proton exchange membrane (PEM) of sulfonated polyethersulfone/ sulfonated graphene oxide (SPES/SGO) to separate the bioanode and biocathode chambers (the details are explained elsewhere [16, 17]). The preparation of PEM was carried out by incorporation of SGO in the polymer matrix of SPES applying the solvent evaporation method. The role of the membrane is to allow proton transfer to complete the cycle of degradation and electricity generation. The FMFC performances are measured by the data assigned to current, voltage, and power density which are displayed in a curve named polarization curve. These data were recorded using a resistance and multimeter Fluke 87. All our experiments were carried out at room temperature.

2.3. Preparation of bioanodes and biocathodes

Bioanodes are electrode system where the electroactive biofilm play the role of catalyzing organic micropollutants degradation i.e. APAP. Due to their low price, carbon-based materials have been chosen as the base material in the bioanodes [18]. 2D-carbon cloth and 3D-carbon felt are among the widely used materials in MFCs. This material serves as the supporting layer for the microorganism biofilm development. In the current study, we utilized four bioanodes namely : CF_1: carbon felt with a pure fungal biofilm of *Trichoderma harzianum*, CF_2: carbon felt with a mixed biofilm of *Trichoderma harzianum*/*Pseudomonas fluorescens*, CC_1: carbon cloth with a pure fungal biofilm of *Trichoderma harzianum*, and CC_2: carbon felt with a mixed biofilm of *Trichoderma harzianum/ Pseudomonas fluorescens*. To prepare the electrodes, rinsing with ultrapure (UP) water and 1M HCl was done as pretreatment. This process was followed by immersing carbon pieces in a mixture of ethanol/ water (1:1) for 10 minutes under sonication and rinsing for 2 min in UP water. Lastly, the electrodes were autoclaved at 120 °C for 15 min before colonization [5]. To chemically activate the carbon cloth, a 1 M H_2SO_4 solution was utilized for 24 hours under stirring conditions [14]. The surface area of CF and CC were 10 cm^2 for both anode and cathode compartments.

To utilize the bioanodes we need to prepare the biofilms. The required biofilm was achieved by successive subcultures on the yeast peptone dextrose adenine (YPDA) medium followed by flooding the agar surface with 20 ml UP water. After filtration, a suspension of microorganisms in UP water was obtained and stored for further biofilm formation on the carbon felt and carbon cloth. Generally, for the fungal biofilm elaboration, the electrodes CF and CC were immersed into a suspension of 10^8 spores.mL^{-1} of *Trichoderma harzianum* for 4 days. Then, a suspension of 10^6 CFU/mL of *Pseudomonas fluorescens* was added with Tryptone Caseine Soja Soup (Fisher scientific Bioblock, France, Lot 00674) to elaborate the mixed biofilms in CC/*Trichoderma harzianum* and CF/*Trichoderma harzianum* bioanodes.

The biocathode was elaborated from a suspension of *Trametes versicolor*. Thereby, the electrodes were immersed into a suspension of 10^7 spores mL^{-1} with PBS and glucose (20 $g.L^{-1}$) for 3 days, before its application in the FMFC. The choice of *Trametes versicolor, a* strain isolated from soil samples in the vicinity of Angers (France), was due to the need of oxygen-reduction biocathode. It has been demonstrated elsewhere that laccases liberated by *T. versicolor* play an important role in catalyzing oxygen reduction reaction [19].

2.4. Electrochemical behavior of APAP

Fig. 1 presents the cyclic voltammograms (CV) of 300 mgL^{-1} APAP in PBS solution, obtained on a glassy carbon electrode (GCE). A well-resolved oxidative peak at a potential of 500 mV/SCE (saturated calomel electrode) [5] and a reduction peak at 100 mV are clearly visible. The oxidative peak is related to the direct oxidation of APAP to N-acetyl-p-benzoquinone imine (NAPQI), with the release of two electrons and protons whereas the reduction peak appears as a result of the reverse reaction (NAPQI → APAP). The inset Fig. 1 displays the calibration curve obtained for

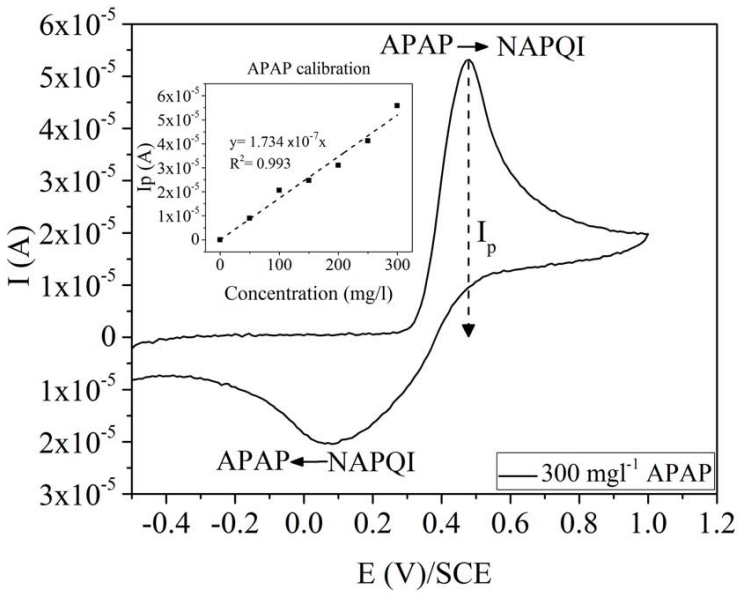

Fig. 1. Cyclic voltammogram of APAP in PBS solution (inset: calibration curve of APAP) (potential scan rate = 100 mV/s, pH =7.2, ionic strength 0.1 M electrode: GCE).

the concentrations of 50 mgL^{-1} to 300 mg L^{-1} of APAP oxidation in PBS solution, illustrating Randles-Sevcik's equation (1) :

$$Ip = 0.1734\ [APAP] \quad (1)$$

where Ip (in μA) and [APAP] (in mgL^{-1}) indicate the current peak and APAP concentration, respectively. The GCE surface needs to be extremely clean and its area well-defined. It is necessary to polish the working electrode of the electrochemical system before each measurement to remove the impurities through mechanical polishing. Here, we applied figure-eight motions using a cloth polishing pad [20].

All the electrochemical analyses were conducted using a PG580 Analyzer (Uniscan Instruments, UK). The employed software was UiEchem version 3.27 (Uniscan Instruments, Biologic company, France). As for the electrochemical cell, a three-electrode conventional type was used including a working electrode (GCE), a counter electrode (platinum and grid), and a reference electrode (SCE). The instruments have been fully explained in a previous study [5].

2.5. Characterization of electrodes

The surface of the unmodified and modified carbon felt and carbon cloth pieces were characterized by a scanning electron microscope with a field emission gun (FEG-SEM) using an LEO 1530 apparatus at a 3 keV acceleration voltage. The samples were covered by an ultra-thin layer of platinum (BAL-TEC MED 020 Balzers Lichentstein evaporating apparatus) with a thickness of 10 nm, in order to increase the quality of the images.

3. RESULTS AND DISCUSSION

3.1. Morphological characterizations of the bioanode

Fig. 2 shows 2D and 3D bioanode materials before and after biofilm formation, i.e., on the first day and after two weeks of the bioanode formation, as observed by SEM. Fig. 2a and d display the clean structure of carbon cloth and carbon felt, respectively. CC is composed of tightly interwoven fibers with a fiber diameter of 8 μm while CF showed the open space between fibers with a diameter of 17 μm. Images Fig. 2b, c, e, and f revealed the formation of biofilm on the surface of carbon felt and carbon cloth after 2 weeks of operation. In theory, carbon felt has a higher specific surface area compared to the carbon cloth, which can explain the higher efficiency of carbon felt. While we should consider that biofilm formation happens on the external surface of fibers and do not penetrate the empty spaces inside the CF.

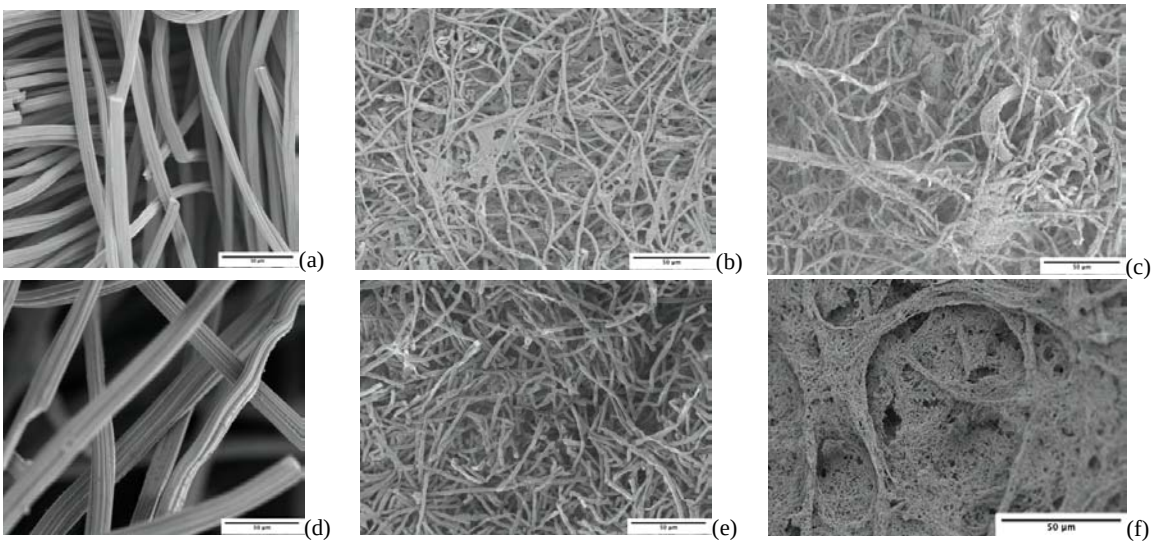

Fig. 2. SEM images of anodes (a: clean CC (magnification x 500), b: *Trichoderma harzianum* biofilm CC (magnification x500), c: mixed biofilm CC (magnification x1000) d: clean CF (magnification x500), e: *Trichoderma harzianum* biofilm CF (magnification x 500); f: mixed biofilm CF (magnification x 500))

This observation is inconsistent with an earlier study in 2019 [21].

3.2. APAP biodegradation

Fig. 3 shows the CV curves of APAP bioelectrochemical degradation for 6 hours in all working reactors with CF_1, modified with *Trichoderma harzianum*, CF_2, modified with *Trichoderma harzianum/Pseudomonas fluorescens*, CC_1, modified with *Trichoderma harzianum* and CC_2, modified with *Trichoderma harzianum/ Pseudomonas fluorescens*. At t=0, a concentration of 300 mgL^{-1} of APAP in PBS solution was injected in the anode compartments of all systems. Then, an initial sample was taken and analyzed by the electrochemical system. The oxidation peak of APAP was monitored in the range of 0.0 to 1.0 V. The sampling was repeated every one hour to compare the degradation behavior for various bioanodes. We have shown a period of 6 hours for all the systems to make it easier to follow the changes (see Fig. 3). Considering the CF_1 and CC_1 in Fig. 3a and b, it is observed that the pure culture of *Trichoderma harzianum* degrades the APAP with no by-products of para-aminophenol (PAP). While in CF_2 and CC_2 (see Fig. 3b and d) respectively) the mixed culture of fungal-bacterial interactions resulted in the apparition of PAP, because of bacterial activity. PAP is a CMR (carcinogenic, mutagenic, and reprotoxic) by-product resulting from the bacterial degradation of APAP [22], which has always been of great concern. During the pure fungal degradation of APAP (CF_1 and CC_1) (see Fig. 3a and c), it is concluded that the complete combustion of APAP has resulted in the production of CO_2 and H_2O. This hypothesis provides us with the fact of fungi's ability to degrade the phenol rings, considered as a milestone achievement in the removal of organic pollutants. So, based on the hypothesis of a complete combustion of APAP, the fungal fuel cell reaction can be written as equation (2) which has been confirmed by an earlier study [1, 5]:

$$C_8H_9O_2N + 37/2\ O_2 \rightarrow 8CO_2 + 9/2\ H_2O + ½\ N_2 \quad (2)$$

If we take a closer look at the CV curves, we can observe a rapid decrease in the current peak (Ip) during the first hour of degradation, which is due to the electrode surface adsorption phenomena of the APAP. This phenomenon was fully discussed elsewhere [23].

3.3. Kinetic analysis

Graphing the obtained data on a logarithmic-linear scale (Fig. 4), with an average regression coefficient

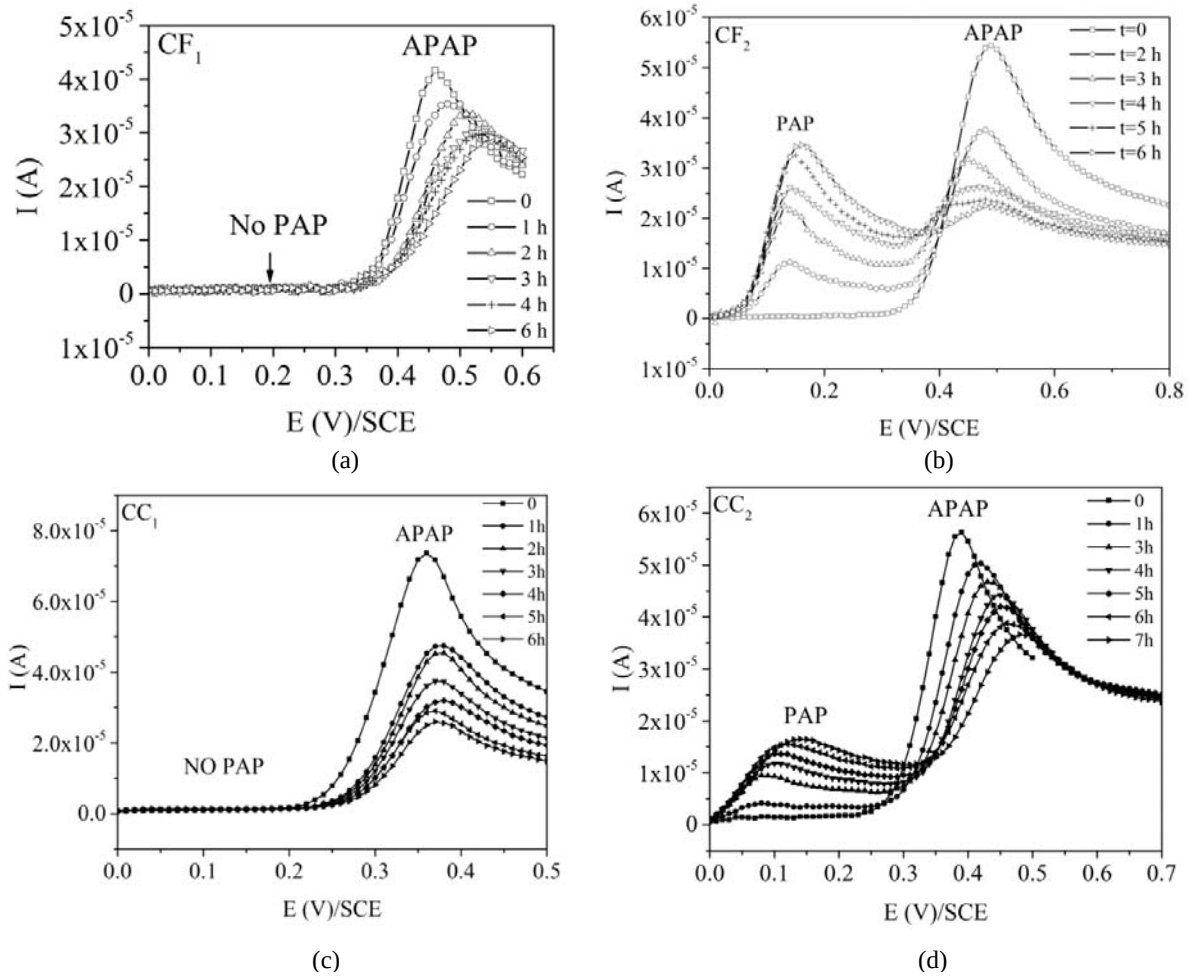

Fig. 3. CV curves of FMFCs working with different bioanodes for 6 hours: a) CF_1 : *Trichoderma harzianum* biofilm, b) CF_2: mixed biofilm *of Trichoderma harzianum/Pseudomonas fluorescens*, c) CC_1: *Trichoderma harzianum* biofilm, and d) CC_2: mixed biofilm of *Trichoderma harzianum/Pseudomonas fluorescens*

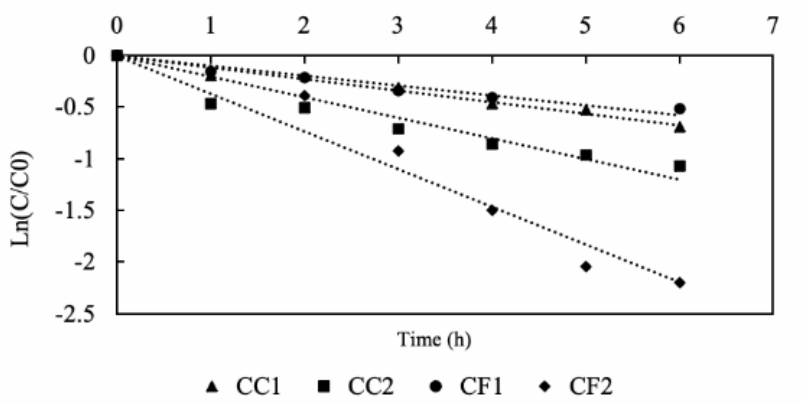

Fig. 4. Kinetic analysis of the APAP biodegradation by bioanodes of CC_1, CC_2, CF_1 and CF_2 (CF_1: modified with *Trichoderma harzianum*, CF_2: modified with *Trichoderma harzianum/Pseudomonas fluorescens*, CC_1: modified with *Trichoderma harzianum* and CC_2: modified with *Trichoderma harzianum/Pseudomonas fluorescens*).

Table 1. Bioanode type, kinetic equation, R^2, and half-life time values of the different bioanodes tested.

Anodes	Kinetic equation	R^2	k (h^{-1})	half-life time (h)
CF_1	$Ln(C/C_0)= -0.096t$	0.98	0.096	7.2
CF_2	$Ln(C/C_0)= -0.366t$	0.97	0.366	1.9
CC_1	$Ln(C/C_0)= -0.113t$	0.99	0.113	6.1
CC_2	$Ln(C/C_0)= -0.200t$	0.98	0.200	3.5

of 0.98, (Table 1), shows that APAP degradation followed a pseudo-first-order reaction. The higher kinetic constant rate of 0.366 and 0.200 is associated with the CF_2 and CC_2 bioanodes, respectively. This was due to the presence of mixed biofilm (see Table 1). The synergic effect of bacterial-fungal interaction led to faster APAP decomposition, although we observed the PAP apparition. However, the pure culture of *Trichoderma harzianum* in both 2D- CC_1 and 3D- CF_1 achieved a very similar kinetic constant of 0.096 and 0.113, respectively. These values represent one third and one half of the value obtained by mixed biofilm bioanodes. It is worth discussing these interesting facts revealed by the results of the half-life time. The half-life time is the required time for the target species to reduce its concentration to half of the initial amount. The half-life time was calculated as 6.1, 3.5, 7.2, and 1.9 hours for CC_1, CC_2, CF_1, and CF_2, respectively. As expected, the shortest half-life of 1.9 h belonged to the CF_2 owning the highest kinetic constant. This is due to the synergic effect of combined bacterial and fungal enzymes activities. From the results, it is clear that there is no significant difference between the performance of CC_1 and CF_1. However, when we added the bacterial biofilm to the culture, 3D-CF_2 degraded the APAP much faster than the 2D-CC_2, suggesting that the bacteria biofilm was well connected to the carbon-based material electrodes.

To our knowledge, very few prior studies have examined the role of MFCs in bioelectrochemical degradation of APAP among which Zhang *et al.* [24] combined the Fenton reaction with the MFCs reporting the maximum APAP degradation of 70%. They also claimed that only 25% of APAP had fully mineralized, and the rest had broken down into para-nitrophenol and para-aminophenol. The half-life reported by the paper was around 4.5 h. In the present study, it is stated that applying the fungal biofilm could result in full mineralization of APAP in a shorter time (See Table 1).

3.4. FMFC performance

The polarization curves associated with the systems are presented in Fig. 5, which shows the power density, current density, and voltage produced by FMFCs applying four bioanodes of CC_1, CC_2, CF_1, and CF_2. As previously mentioned, MFCs are promising tools for the production of clean energy together with pollution removal. The electrons produced as a result of APAP biodegradation. Then, electrons pass through the electric circuit to reach the cathode. In the cathode compartment, the electrons are combined with the protons diffusing from the anode through the membrane, and oxygen which is provided externally [25]. This results in the production of water molecules in the cathode. The movements of electrons produce current as well as generate the electricity defined in terms of power density. Here, we report the power density and current density, which are the amount of power (P) and current (I) divided by the electrode surface area. The aim was to provide the possibility of simply comparing the results obtained with each other and also with other studies.

Generally, it is notable that the mixed biofilm bioanodes (CF_2 and CC_2) (see Fig. 5b and d) produced higher power density than their pure fungal biofilms (CF_1 and CC_1, respectively) (see Fig. 5a and c) regardless of the material types. This might be related to their higher degradation rate and the ability to consume APAP fast. The highest value belongs to CF_2 followed by CF_1, CC_2, and finally CC_1. The power density of CF_2 with the value of 1.7 mW m^{-2} is 13 times higher than CF_1 (0.13 mW m^{-2}), and that of CF_1 itself is almost

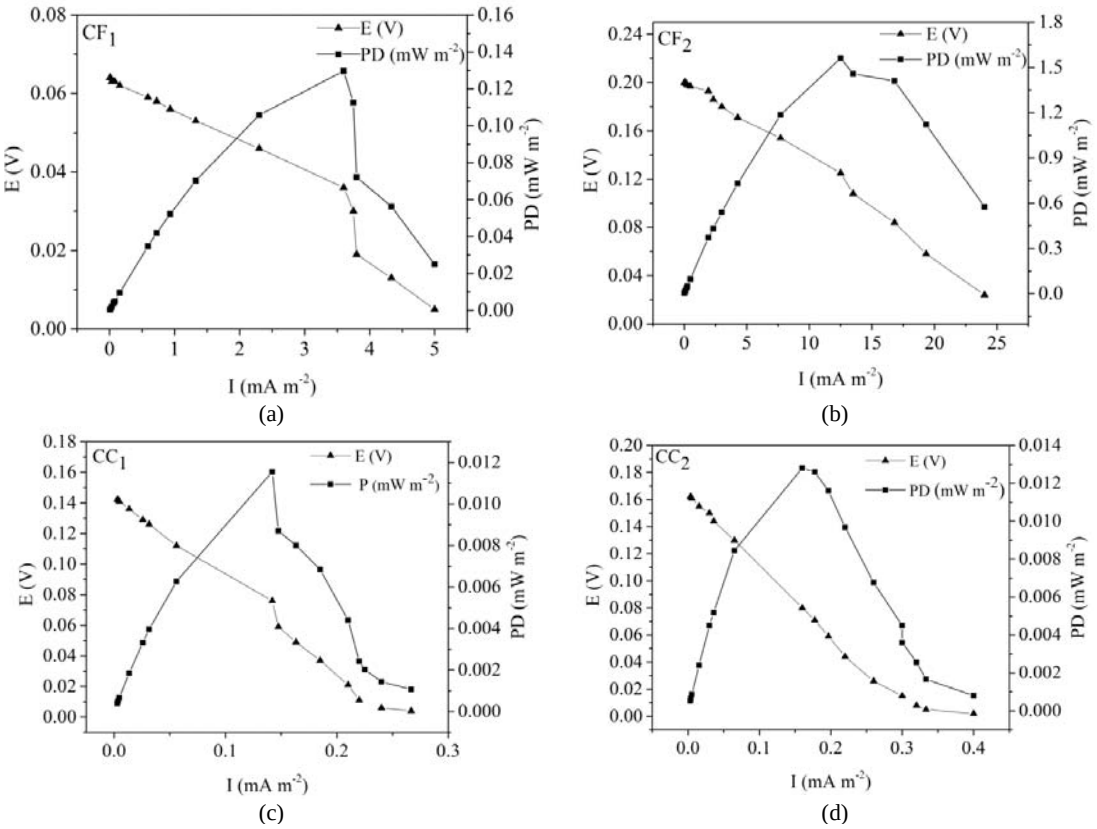

Fig. 5. Polarization curves of all FMFCs working with four bioanodes; a) CF_1: modified with *Trichoderma harzianum*, b) CF_2: modified with *Trichoderma harzianum/Pseudomonas fluorescens*, c) CC_1: modified with *Trichoderma harzianum* and d) CC_2: modified with *Trichoderma harzianum/Pseudomonas fluorescens*.

10 times higher than CC_2 with the value of 0.013 mW m^{-2}. CC_1 showed the lowest power density of 0.011 mW m^{-2}. The results of the experiments found clear support for the idea that 3D carbon felts are better choices for the FMFCs in terms of electron transfer efficiency and energy production. On the contrary, other studies have shown that 2D and 3D carbon materials were similarly efficient in terms of current density. They have applied the 2D CC and 3D CF as bioanodes for food waste treatment and concluded that considering the biofilm pattern in the case of chemical-rich solution, 2D carbon cloth could equally perform as 3D porous carbon felt [15].

4. CONCLUSION

This paper compared the performance of the 2D carbon cloth and 3D carbon felt in terms of FMFC performance (power density) and APAP biodegradation rate. We applied two biofilm populations for each type of electrode including the pure culture of *Trichoderma harzianum* and mixed culture of *Trichoderma harzianum/Pseudomonas fluorescens.* This resulted in four bioanodes of CC_1, CC_2, CF_1, and CF_2, providing us with the perspective of better performance for mixed biofilm in terms of power density for both carbon felt and carbon cloth. We also concluded that while applying the pure fungal culture, both materials showed similar efficiency for APAP biodegradation, regardless of the electrode type. Besides, these findings provide additional information about the FMFC, as 3D-carbon felts covered with pure fungal or bacterial-fungal biofilm showed much higher efficiency in terms of electron transfer and current production compared to 2D carbon cloth. This paper provides a good starting point for discussion and further research on the role of synergistic association of microorganisms in connection to the supportive layer electrode and how synergistic behavior could be managed to improve the FMFC performances. Furthermore, future comprehensive studies are required to investigate the enzymes produced by

the microorganisms (bacteria and fungi) to better manage their performance in correlation to the generation of higher power densities. Also, more studies are suggested to follow the biofouling phenomena in the membrane due to the presence of microorganisms.

ACKNOWLEDGMENTS

We thank Romain Mallet and Florence Manero from microscopy center of the university of Angers (SCIAM). Sincere thanks to the French embassy in Tehran (Mr. J. C. BONTE) and Campus France for the french/Iranian research PhD grant program and funds attributed to the research project of Mrs. SHABANI for 8 months internship in France (Dec. 2019 to July 2020). The authors gratefully acknowledge the financial support from the Iran National Science Foundation (Grant No. 97014305) and the Ministry of Science and Technology of Iran for the funds allocated to the PhD thesis of Mrs. SHABANI. Lots of thanks to the review by a native English speaker and to Oceane Pontie, Bachelor student in the University of Angers for her help.

CONFLICT OF INTEREST STATEMENT

The authors declare that they have no conflict of interest.

REFERENCES

1. López Zavala, M. Á. and Jaber Lara, C. R. 2018, Environ. Eng. Sci., 35, 1248-1254.
2. Fatta-Kassinos, D., Meric, S. and Nikolaou, A. 2011, Anal. Bioanal. Chem., 399, 251-275.
3. Hu, J., Zhou, L., Zhou, Q., Wei, F., Zhang, L. and Chen, J. 2012, Adv. Mater. Res., 441, 531-535.
4. Singh, R. K., Tripathi, R. Ranjan, A. and Srivastava, A. K. 2020, in Abatement of Environmental Pollutants, Elsevier, 177-191.
5. Pontié, M., Jaspard, E., Friant, C., Kilani, J., Fix-Tailler, A., Innocent, C., Chery, D., Mbokou, S. F., Somrani , A., Cagnon, B. and Pontalier, P. Y. 2019, Biocatal. Agric. Biotechnol., 22, 101376.
6. Mbokou, S. F., Tonle, I. K. and Pontié, M. 2017, J. Appl. Electrochem., 47, 273-280.
7. Birjandi, N., Younesi, H., Ghoreyshi, A. A. and Rahimnejad, M. 2016, J. Environ. Manage., 180, 390-400.
8. Li, S., Cheng, C. and Thomas, A. 2017, Adv. Mater., 29, 1602547.
9. Chen, S., He, G., Hu, X., Xie, M., Wang, S., Zeng, D., Hou, H. and Schröder, U. 2012, ChemSusChem., 5, 1059-1063.
10. Guo, K., Soeriyadi, A. H., Patil, S. A., Prévoteau, A., Freguia, S., Gooding, J. J. and Rabaey, K. 2014, Electrochem. commun., 39, 1-4.
11. Chen, S., He, G., Carmona-Martinez, A. A., Agarwal, S., Greiner, A., Hou, H. and Schröder, U. 2011, Electrochem. commun., 13, 1026-1029.
12. Sleutels, T. H. J. A., Lodder, R., Hamelers, H. V. M. and Buisman, C. J. N. 2009, Int. J. Hydrogen Energy, 34, 9655-9661.
13. Kipf, E., Zengerle, R., Gescher, J. and Kerzenmacher, S. 2014, ChemElectroChem, 1, 1849-1853.
14. Chen, S., Liu, Q., He, G., Zhou, Y., Hanif, M., Peng, X., Wang, S. and Hou, H. 2012, J. Mater. Chem., 22, 18609-18613.
15. Blanchet, E., Erable, B., De Solan, M.-L. and Bergel, A. 2016, Electrochem. commun., 66, 38-41.
16. Shabani, M., Younesi, H., Rahimpour, A. and Rahimnejad, M. 2019, Biocatal. Agric. Biotechnol., 22, 101369.
17. Shabani, M., Younesi, H., Pontié, M., Rahimpour, A., Rahimnejad, M. and Zinatizadeh, A. A. 2020, J. Clean. Prod., 98, 121446.
18. Slate, A. J., Whitehead, K. A., Brownson, D. A. C. and Banks, C. E. 2019, Renew. Sustain. Energy Rev., 101, 60-81.
19. Le Goff, A., Holzinger, M. and Cosnier, S. 2015, Cell. Mol. Life Sci., 72, 941-952.
20. Elgrishi, N., Rountree, K. J., McCarthy, B. D., Rountree, E. S., Eisenhart, T. T. and Dempsey, J. L. 2018, J. Chem. Educ., 95, 197-206.
21. Roubaud, E., Lacroix, R., Da Silva, S., Etcheverry, L., Bergel, A., Basséguy, R. and Erable, B. 2019, Front. Energy Res., 7.
22. Mbokou, S. F., Pontié, M., Razafimandimby, B., Bouchara, J. P., Njanja, E. and Tonle Kenfack, I. 2016, Anal. Bioanal. Chem., 408, 5895-5903.
23. Elgrishi, N., Rountree, K. J., McCarthy, B. D., Rountree, E. S., Eisenhart, T. T. and Dempsey, J. L. 2018, J. Chem. Educ., 95, 197-206.
24. Zhang, L., Yin, X. and Li, S. F. Y. 2015, Chem. Eng. J., 276, 185-192.
25. Logan, B. E., Hamelers, B., Rozendal, R., Schröder, U., Keller, J., Freguia, S., Aelterman, P., Verstraete, W. and Rabaey, K. 2006, Environ. Sci. Technol., 40, 5181-5192.